Opposing mechanisms mediate morphine- and cocaine-induced generation of silent synapses

Nicholas M. Graziane[1,2], **Shichao Sun**[1,5], **William J. Wright**[1,5], **Daniel Jang**[1], **Zheng Liu**[2], **Yanhua H. Huang**[2], **Eric J. Nestler**[3], **Yu Tian Wang**[4], **Oliver M. Schlüter**[1], and **Yan Dong**[1,2]

[1]Department of Neuroscience, University of Pittsburgh, Pittsburgh, PA 15260

[2]Department of Psychiatry, University of Pittsburgh, Pittsburgh, PA 15219

[3]Fishberg Department of Neuroscience and Friedman Brain Institute, Icahn School of Medicine at Mount Sinai, New York, NY 10029

[4]Brain Research Centre and Department of Medicine, Vancouver Coastal Health Research Institute, University of British Columbia Vancouver, BC, Canada

Summary

Exposures to cocaine and morphine produce similar adaptations in nucleus accumbens (NAc)-based behaviors, yet produce very different adaptations at NAc excitatory synapses. Here, we explain this paradox by showing that both drugs induce NMDA receptor-containing, AMPA receptor (AMPAR)-silent excitatory synapses, but in distinct cell types through opposing cellular mechanisms: cocaine selectively induces silent synapses in D1-type neurons likely via a synaptogenesis process, whereas morphine induces silent synapses in D2-type neurons via internalization of AMPARs from pre-existing synapses. After drug withdrawal, cocaine-generated silent synapses become 'unsilenced' by recruiting AMPARs to strengthen excitatory inputs to D1-type neurons, while morphine-generated silent synapses are likely eliminated to weaken excitatory inputs to D2-type neurons. Thus, these cell-type specific, opposing mechanisms produce the same net shift of the balance between excitatory inputs to D1- and D2-type NAc neurons, which may underlie certain common alterations in NAc-based behaviors induced by both classes of drugs.

Keywords

morphine; cocaine; accumbens; silent synapse; D1 receptor; D2 receptor

Corresponding Authors: Dr. Yan Dong, Dept. Neuroscience, Univ. of Pittsburgh, A210 Langley Hall / 5th & Ruskin Ave, Pittsburgh, PA 15260, yandong@pitt.edu, Phone: 412-624-3140.
[5]These authors contributed equally to this manuscript

Introduction

Exposure to drugs of abuse reshapes future behaviors partially by altering excitatory synapses in the nucleus accumbens (NAc)[1]. However, despite triggering many similar NAc-based behavioral consequences such as locomotor sensitization, conditioned reward, and self-administration and relapse, exposure to stimulant versus opiate drugs induces distinctly different adaptations at NAc excitatory synapses. This cellular-behavioral disconnection is strikingly exemplified in cocaine- and morphine-exposed rodents, in which the density of dendritic spines, postsynaptic structures of excitatory synapses, is increased in the NAc after withdrawal from cocaine but decreased after withdrawal from morphine[2,3]. These opposite synaptic consequences, which may represent new synapse formation and synapse elimination, respectively[4,5], raise two questions: How are the opposing synaptic modifications achieved by cocaine and morphine? And do the opposing synaptic modifications result in similar or contrasting functional alterations of the NAc?

To address these questions, we focus on drug-induced generation of silent synapses. Silent glutamatergic synapses contain functional NMDA receptors (NMDARs), with AMPA receptors (AMPARs) either absent or highly labile[6,7]. In theory, silent synapses can be generated either by delivering NMDARs to new synaptic locations or internalizing AMPARs from pre-existing synapses, and they can subsequently be either stabilized by recruiting AMPARs or eliminated by synapse turnover[6,7]. Previous results show that exposure to cocaine generates silent synapses in the NAc shell (NAcSh) by synaptic insertion of new NMDARs[8–10]. Further analyses indicate that cocaine-generated silent synapses share core features of nascent synapses, likely corresponding to cocaine-induced, newly generated dendritic spines[4,5,11]. Our present results support a scheme whereby exposure to morphine also generates silent synapses in the NAcSh, but through internalization of AMPARs from pre-existing synapses. Furthermore, while cocaine-induced generation of silent synapses occurs preferentially in dopamine D1 receptor-expressing (D1R) medium spiny neurons (MSNs) in the NAcSh, morphine-induced silent synapses are enriched in D2R MSNs. After withdrawal, a portion of cocaine-generated silent synapses matured by recruiting AMPARs to strengthen glutamatergic input to D1R MSNs, whereas morphine-generated silent synapses are likely pruned away, resulting in weakened glutamatergic input to D2R MSNs. In several rodent models of drug of addiction, D1R and D2R NAcSh MSNs mediate opposing behavioral effects[12–14]. Thus, the opposing but cell type-specific synaptic modifications triggered by exposure to cocaine versus morphine both increase the ratio of excitatory inputs to D1R over D2R MSNs, potentially leading to the same functional shift of the NAc and thereby to common NAc-based behavioral adaptations.

Results

Exposure to morphine generates silent synapses

We previously demonstrated that repeated exposure to cocaine (i.p. injection, 15mg/kg/d for 5d, 1d withdrawal) generated silent synapses in NAcSh MSNs in rats[8,11]. In this study, we observed that exposure to morphine, with a dosing regimen (i.p. 10mg/kg/d for 5d, 1d withdrawal) that typically induces locomotor sensitization and conditioned place

preference[15,16], also generated silent synapses in NAcSh MSNs. Specifically, we first compared the trial-to-trial coefficient of variation (CV) of AMPAR- and NMDAR-mediated excitatory postsynaptic currents (EPSCs), which were isolated at −70 and +50mV, respectively, and measured based on their distinct kinetics (Fig. 1a). CV is generally inversely proportional to the number of functional synapses and their release probability[17]. Thus, for a given set of synapses mixed with silent (NMDAR-only) and nonsilent synapses, the total number of NMDAR-containing synapses (measured at +50mV) should be greater than the number of AMPAR-containing synapses (measured at −70mV; NMDAR-only synapses are blocked by Mg^{2+} at this voltage), resulting in reduced ratio of CV of NMDAR EPSCs to CV of AMPAR EPSCs. After 1d withdrawal from morphine, the CV-NMDAR/CV-AMPAR ratio was significantly decreased in NAcSh MSNs in rats (Fig. 1b–d). It is unlikely that a depolarization-induced suppression of presynaptic release may have contributed to the decrease in CV, as a reduction of release probability would predict an increase, rather than a decrease, in CV at depolarized membrane potentials. Thus, these results suggest the possibility that exposure to morphine generates silent synapses in these neurons.

We next used the minimal stimulation assay, in which low intensity stimulations were applied to a small number of synapses, eliciting intermittent successful or failed EPSCs over the trials. Because silent synapses only respond to presynaptic transmitter release at depolarized membrane potentials but not at near resting potentials due to Mg^{2+} block of NMDARs, the failure rate at −70mV should be higher than at +50mV if silent synapses are included in the recordings. Based on the different failure rates at these two membrane potentials, the percentage of silent synapses among all recorded synapses (% silent synapses) can be assessed with the assumptions that the presynaptic release sites are independent and that the release probabilities across all synapses are equal[8,18]. The minimal stimulation assay revealed that, after 1d withdrawal from cocaine or morphine, % silent synapses was significantly increased in NAcSh MSNs in young (~50d old) rats and in older (70–80d old) rats (Fig. 1e–i). Similar to cocaine exposure[8], % silent synapses increased gradually over the 5d morphine exposure, and returned to basal levels after 7d withdrawal (Fig. 1i). These results suggest that, similar to cocaine, exposure to morphine also generates AMPAR-silent synapses in NAcSh MSNs.

Morphine generates silent synapses via AMPAR internalization

Cocaine-induced generation of silent synapses is accompanied by synaptic insertion of GluN2B-containing NMDARs[8,11]. These and other features suggest that cocaine-generated silent synapses are newly formed[4,5]. Consistent with this hypothesis, we observed prolonged decay kinetics of NMDAR EPSCs in rat NAcSh MSNs 1d after cocaine administration, and increased sensitivity of NMDAR EPSCs to the GluN2B-selective antagonist Ro256981 (200nM), suggesting an increase in the relative weight of synaptic GluN2B NMDARs (Fig. 2a–d). However, such changes were not detected after morphine exposure, suggesting that morphine-induced generation of silent synapses is not mediated by insertion of GluN2B NMDARs to new synapses (Fig. 2a–d).

We then examined whether morphine-induced generation of silent synapses was mediated by internalization of AMPARs from pre-existing synapses. We injected the rats intravenously with a Tat-GluA2$_{3Y}$ peptide each time they received cocaine or morphine (see **Methods**). GluA2-containing AMPARs are enriched at NAc excitatory synapses[19]. The synthetic Tat-tagged peptide (^{869}YKEGYNVYG^{877}) can translocate into neurons and block experience-dependent AMPAR endocytosis with minimal effects on constitutive AMPAR trafficking or basal synaptic transmission[20], and these functional specificities have been confirmed in NAc MSNs[21]. Co-administration of the control (scrambled) peptide Tat-GluA2 (VYKYGGYNE) (1.5 nmol/g), which does not affect AMPAR trafficking[21], did not affect the basal level of silent synapses (in saline-exposed rats), and did not affect cocaine- or morphine-induced generation of silent synapses in NAcSh MSNs (Fig. 2e,f). However, co-administration of Tat-GluA2$_{3Y}$ (1.5 nmol/g), which prevents AMPAR internalization, prevented morphine- but not cocaine-induced generation of silent synapses (Fig. 2g,h). Note that Tat-GluA2$_{3Y}$ treatment appears to also lower % silent synapses in cocaine-exposed rats, suggesting additional mechanisms for cocaine-induced generation of silent synapses (see **Discussion**). Collectively, these results suggest that opposing mechanisms, namely insertion of NMDARs to new synapses versus internalization of AMPARs from pre-existing synapses, are employed by cocaine versus morphine, respectively, to generate silent synapses in the NAcSh.

Morphine-induced spine elimination in rats

Cocaine-induced generation of silent synapses in the NAcSh is accompanied by an increased density of MSN spines, and a molecular manipulation that prevents cocaine-induced generation of silent synapses prevents cocaine-induced increase in spine density[11]. These and other results lead to a speculation that cocaine-generated silent synapses are new synapses and new spines of NAc MSNs[4]. On the other hand, the MSN spine density is decreased after morphine withdrawal[2], and AMPAR internalization-mediated generation of silent synapses can be an initial step toward synapse/spine elimination. We therefore used the peptides verified above to explore the relationship between cocaine/morphine-generated silent synapses and spine morphology. The rats were injected with Tat-GluA2$_{3Y}$ or scrambled peptide intravenously each time they received cocaine or morphine (see **Methods**).

Using DiI staining[22], we focused on secondary dendrites of rat NAcSh MSNs, which densely express at least four types of spines[2,3]: filopodia-like spines, which are long dendritic protrusions without apparent heads; mushroom-like spines, which are protrusions with a diameter of spine heads >2x of their necks; long-thin spines, which are protrusions with spine heads 1–2 times larger in diameter than their necks; and stubby spines, which are short and thick protrusions without detectable heads (Fig. 3a–d). While not absolute, a heuristic theme of spine morphology is that mushroom-like spines are more mature and stable postsynaptic structures enriched in AMPARs, whereas filopodia-like and long-thin spines are transitional postsynaptic structures with shorter life times and fewer or no AMPARs[23].

1d after cocaine administration, we observed a significant increase in total spine density on rat NAcSh MSNs, as reported previously[3,11] (Fig. 3e,f), and this increase appears to be primarily attributable to increases in filopodia-like and long-thin spines, but not mushroom-like or stubby spines (Fig. 3g–j). These effects were intact when scrambled peptide or GluA2$_{3Y}$ was co-administered with cocaine (Fig. 3e–j), suggesting that cocaine-induced spinogenesis was independent of AMPAR internalization.

In stark contrast, total spine density on NAcSh MSNs was not altered 1d after morphine administration (p=1.0), but, importantly, the proportion of filopodia-like spines was significantly increased and the proportion of long-thin spines was decreased, suggesting a conversion of long-thin spines to filopodia-like spines (Fig. 3e–j). These potential spine-weakening effects were prevented when GluA2$_{3Y}$, but not scrambled peptide, was co-administered with morphine (Fig. 3e–j), suggesting an essential role of AMPAR internalization in this process.

21–28d after cocaine administration, the cocaine-induced increase in total spine density on NAcSh MSNs persisted, and this increase was not only attributable to increases in filopodia-like and long-thin spines, but also mushroom-like spines (Fig. 4). Thus, some immature spines were strengthened and matured after cocaine withdrawal. These effects of cocaine were intact in rats that were co-administered GluA2$_{3Y}$ during cocaine exposure (Fig. 4).

In contrast, 21–28d after morphine administration, total spine density on NAcSh MSNs was significantly decreased, which was primarily attributable to the loss of long-thin spines (Fig. 4). These results suggest that some weakened spines observed 1d after morphine administration were eliminated after long-term withdrawal. Furthermore, co-administration of GluA2$_{3Y}$ during morphine exposure prevented all these effects observed 21–28d after morphine withdrawal (Fig. 4), suggesting that preventing the initial AMPAR internalization and synaptic weakening prevents subsequent synapse elimination after morphine withdrawal.

Silent synapse-based remodeling of NAc circuits

Transgenic mice were used in subsequent experiments to examine cell type-specific expression of silent synapses and behavioral consequences. We therefore used mice to perform the same experiments as described in Figures 3 and 4, and detected similar effects of cocaine and morphine on NAcSh MSN spines (Fig. 5). These data confirm that preventing AMPAR internalization prevents morphine-induced spine elimination.

Do the opposing processes of cocaine- and morphine-induced generation of silent synapses lead to the same or different functional alterations in the NAcSh? To address this question, we examined cocaine- and morphine-induced generation of silent synapses in D1R and D2R NAcSh MSNs using a mouse line in which D1R MSNs are genetically tagged with tdTomato[24]. Using genetically labeled mice, previous studies indicate that the presence and absence of fluorescence signals predict D1R versus D2R MSNs[24,25]. 1d after the 5d drug procedure, % silent synapses in tdTomato-positive (+) NAcSh MSNs (operationally defined as D1R MSNs) was increased in cocaine-exposed mice but not in morphine-exposed mice (Fig. 6a,b). In contrast, % silent synapses in tdTomato-negative (−) MSNs (operationally

defined as D2R MSNs) was not significantly affected in cocaine-exposed mice but was increased in morphine-exposed mice (Fig. 6e,d). Thus, exposure to cocaine versus morphine preferentially generates silent synapses in NAcSh D1R and D2R MSNs, respectively.

If cocaine-induced generation of silent synapses involves a synaptogenesis-like process, the potential maturation of these silent synapses by recruiting AMPARs after prolonged withdrawal should strengthen the overall excitatory synaptic strength in D1R NAcSh MSNs. On the other hand, if morphine-induced generation of silent synapses is a transition toward synapse elimination, the potential elimination after prolonged withdrawal should weaken the overall excitatory synaptic strength in D2R NAcSh MSNs. These changes would thus lead to a common circuitry consequence: an increase in the ratio between excitatory synaptic inputs to D1R MSNs over D2R MSNs after prolonged drug withdrawal. To test this possibility, we simultaneously recorded EPSCs from D1R and D2R NAcSh MSNs in response to the same presynaptic stimulation after 21d withdrawal from cocaine or morphine exposure. On average, the single stimulation should normalize presynaptic factors, allowing the dual recording to reveal potentially different excitatory synaptic strengths in D1R versus D2R MSNs (Fig. 6e). Upon the same presynaptic stimulation, EPSCs were elicited in both D1R and D2R MSNs (Fig. 6f). The ratio of excitatory inputs to D1R over D2R MSNs ($EPSC_{D1}/EPSC_{D2}$), which was measured by the peak amplitudes of EPSCs in D1R MSNs over the peak amplitudes of EPSCs in D2R MSNs, was significantly increased in both cocaine- and morphine-exposed mice (Fig. 6f,g).

Behavioral correlates

D1R and D2R NAc MSNs play distinct roles in drug-induced locomotor responses and drug-conditioned learning[13,26]. The above results suggest that co-administration of $GluA2_{3Y}$ prevented silent synapse-mediated synaptic weakening selectively in D2R MSNs following exposure to morphine. We therefore used the $GluA2_{3Y}$-based manipulations to explore the role of this cell type-specific synaptic remodeling in both morphine-induced and cocaine-induced locomotor responses and conditioned place preference (CPP).

In locomotor tests, mice with co-administration of $GluA2_{3Y}$, scrambled peptide, or without co-administration of a peptide similarly exhibited progressively increased locomotor responses during the 5d morphine procedure (10mg/kg/d), compared to saline-injected mice (Fig. 7a,b). Likewise, 21d after the 5d procedure, a challenge injection of morphine (10mg/kg) induced similar locomotor responses in all morphine-exposed mice, including mice receiving co-administration of $GluA2_{3Y}$, scrambled peptide, or no peptide (Fig. 7c). Similar to morphine, a challenge injection of cocaine (15mg/kg) on 21d after the 5d cocaine procedure (15mg/kg/d) induced similar locomotor responses in mice with co-administration of $GluA2_{3Y}$, scrambled peptide, or no peptide during the 5d procedure (Supplementary Fig. 1a,b). We next examined the acute effects of $GluA2_{3Y}$ on cocaine- or morphine-induced locotmor responses. 21d after the 5d cocaine or morphine procedure without co-administration of $GluA2_{3Y}$ (Supplementary Fig. 1c,d,f), mice were given $GluA2_{3Y}$ or scrambled peptide, followed by a challenge injection of cocaine (15mg/kg) or morphine (10mg/kg), respectively. The challenge drug-induced locomotor responses were similar in mice with co-administered $GluA2_{3Y}$ or scrambled peptides in both cocaine- and morphine-

exposed mice (Supplementary Fig. 1e,g). Collectively, these results suggest that AMPAR internalization-mediated generation of silent synapses is not required for cocaine- or morphine-induced locomotor responses.

In CPP tests, mice received daily, alternating conditioning for 40min both with drug (saline control, cocaine, or morphine) and with saline, separated by 6h, for 5d (Fig. 7d; also see Methods). Immediately before the chamber pairing, mice received bilateral intra-NAcSh administration of $GluA2_{3Y}$ or scrambled peptide. 21d after the 5d conditioning (d28), the mice spent significantly more time in the cocaine- or morphine-paired chambers compared to before conditioning. The increase of time in drug-paired chambers was similar in cocaine-exposed mice treated with $GluA2_{3Y}$ or scrambled peptide, indicating that preventing AMPAR internalization-mediated generation of silent synapses did not prevent cocaine-induced CPP (Fig. 7e). However, morphine-induced CPP was selectively disrupted in $GluA2_{3Y}$-, but not scrambled peptide-, administered mice (Fig. 7e). These results suggest that silent synapse-based remodeling of NAcSh circuits is required for morphine-conditioned learning.

Discussion

Our present results show that silent synapses can be intermediate, transitional structures in both synapse formation and elimination; they are utilized after exposure to cocaine versus morphine to differentially remodel excitatory inputs to NAcSh MSNs, resulting in similar circuitry consequences. These results can explain some of the common behavioral responses to stimulant and opiate classes of addictive drugs in the face of very different molecular-cellular adaptations.

Generation and elimination of spines and synapses

After long-term withdrawal from cocaine or morphine, increased or decreased spine densities are observed, respectively, in the NAc[2,3], indicating opposing synaptic remodeling. The morphine-induced decrease in spine density may represent synapse elimination, and our results suggest that this process is achieved through two steps, the initial silencing/weakening of existing synapses via internalization of AMPARs, followed by pruning of silent/weakened synapses. Abundant in the developing brain, silent synapses are often nascent, immature synapses; they are highly unstable, and can either mature/stabilize upon frequent use or be eliminated if not used[6,7]. Thus, synapse formation, maturation, and elimination are connected mechanisms that function coordinately to form new circuits and craft them from generalized connections into dedicated ones during brain development. In light of this, we hypothesize that developmental mechanisms of synapse elimination are awakened after morphine exposure, and generation of silent synapses is the first step toward synapse elimination.

Internalization of AMPARs

Reflecting morphine-induced generation of silent synapses, the CV of AMPAR EPSCs was increased relative to the CV of NMDAR EPSCs (Fig. 1), suggesting decreased AMPAR-mediated responses. Furthermore, $GluA2_{3Y}$, which selectively blocks experience-dependent

endocytosis of GluA2-containing AMPARs with minimal effects on constitutive AMPAR trafficking, prevented morphine-induced generation of silent synapses (Fig. 2). These results suggest that morphine-induced generation of silent synapses is mediated by internalization of AMPARs from pre-existing synapses, likely through experience-dependent synaptic plasticity (e.g., LTD). Experience-dependent synaptic plasticity is highly pathway-specific—only synapses that are activated by experience are subject to plastic changes. Thus, it is reasonable to postulate that the primary pharmacological effects of morphine on AMPAR internalization[27] together with the circuit-specific effects of morphine-induced emotional and motivational experience produce cell type-specific generation of silent synapses.

Although our previous and current results suggest that cocaine-induced generation of silent synapses is predominately mediated by insertion of GluN2B NMDARs to new synapses, these results do not rule out the possibility that a portion of silent synapses, likely in certain types of neurons or within certain projections, are generated through internalization of AMPARs. Indeed, recent results suggest that within ~3% of NAc neurons that are activated by cocaine re-exposure after cocaine withdrawal, silent synapses are generated independent of GluN2B NMDARs, and likely through internalization of AMPARs[28]. Echoing this finding, although GluA2$_{3Y}$ did not prevent cocaine-induced generation of silent synapses, the level of cocaine-generated silent synapses was lower in GluA2$_{3Y}$-treated rats than in control rats (14% vs. 23%; Fig. 2f,h). Thus, exposure to cocaine or morphine likely triggers both synaptogenesis and synapse elimination processes—at different synapses, within different afferents, or in different cell types, with synaptogenesis effects predominating in cocaine-exposed animals and synapse elimination effects predominating in morphine-exposed animals. In either case, generation of silent synapses can serve as a transitional step to achieve the ultimate synaptic remodeling, i.e., synapse formation or elimination.

Silent synapses and dendritic spines

Our present results show that the densities of thin spines, including filopodia-like or long-thin spines, increased upon drug-induced generation of silent synapses, and declined to basal levels upon disappearance of silent synapses. Furthermore, administration of GluA2$_{3Y}$, which prevented morphine-induced generation of silent synapses, prevented morphine-induced increases in thin spines. These correlative results suggest that the increased thin spines are likely the neuronal substrates of drug-generated silent synapses. This notion is consistent with several key features of thin dendritic spines demonstrated previously.

First, while a small number of nonsynaptic spines exist[29], and mushroom-like spines tend to have better-defined presynaptic boutons[30,31], extensive evidence shows that even the thinnest spines often express signature synaptic proteins, make synapses with presynaptic boutons, and respond functionally to locally uncaged glutamate[32–35]. Thus, most drug-generated thin spines are likely postsynaptic structures of true synapses.

Second, it has been consistently observed that the volume of the spine head is positively correlated with the size of the postsynaptic density and the content of AMPARs[23,36], with AMPARs abundant in mushroom-like spines but sparse or absent in long-thin and filopodia-like spines[37]. In contrast, the number of NMDARs is much less dependent on spine size[36,38,39]. Thus, compared to mushroom-like spines, a portion of thin spines is more likely

to be the neuronal substrates of silent synapses in the NAcSh after short-term withdrawal from cocaine or morphine.

Third, although the currently used categorization of dendritic spines is heuristic with respect to understanding their structure-function relationship, extensive EM studies show that dendritic spines constitute a structural continuum rather than clear-cut categories[23]. Particularly for thin spines, it is most likely that they are a mixture of AMPAR-absent and AMPAR-sparse synapses; these two populations of synapses are morphologically similar but functionally distinct. As such, although thin spines in cocaine- and morphine-preexposed animals share morphological similarities, they may have different receptor compositions, functionalities, or cellular fates.

Forth, time-lapse studies in the neocortex show that while some thin spines are persistent, the majority of thin spines are transient, either disappearing or stabilizing into mushroom-like spines[40]. These results suggest that most thin spines are intermediate structures, mediating the transmission from weak, newly generated synapses toward matured synapses, or from matured synapses toward weak synapses that can be eventually eliminated. Our results show that morphine-generated thin spines disappeared after withdrawal, with the time course approximately consistent with the disappearance of silent synapses (Figs. 3,4). These transient thin spines may correspond to morphine-generated silent synapses. After 21d withdrawal from cocaine, however, the density of thin spines remained high, despite the disappearance of silent synapses (Figs. 1,3,4). We speculate that during cocaine withdrawal, some thin spines have already recruited AMPARs but morphologically remain thin. This speculation is consistent with the in vivo analysis of the adult somatosensory cortex, in which, unlike in vitro preparations[41], the time course of final spine maturation lasts for days to weeks[34].

Balance between D1R and D2R circuits

D1R- and D2R MSNs are the two major neuronal subtypes in the NAc with distinct, and often opposing, circuitry and behavioral functions[13,26,42]. Previous studies showed a monomodal distribution of % silent synapses across randomly recorded NAcSh MSNs in cocaine-exposed rats, suggesting that exposure to cocaine generates silent synapses in both D1R and D2R MSNs[11]. Using D1-tdTomato mice, our present study revealed a clear separation between D1R and D2R MSNs in cocaine- and morphine-induced generation of silent synapses. In addition, we did not detect substantially higher % silent synapses in D1R or D2R MSNs in cocaine- or morphine-exposed mice (Fig. 6) than in randomly sampled MSNs in rats (Fig. 1). These seemingly discrepant results may be reconciled by two technical considerations. First, the estimated % silent synapses in drug-exposed animals is the sum of basal and drug-generated silent synapses, thus not exclusively attributable to drug effects. As such, an increase in the drug-generated portion does not result in the same magnitude of increase in overall % silent synapses, particularly in certain experimental conditions in which the basal silent synapse levels are high. Second, when the data for D1R and D2R MSNs in Figure 6 were pooled together as total NAcSh MSNs, the % silent synapses was still significantly higher after exposure to cocaine or morphine (saline, 8.0±3.1%; cocaine, 27.6±4.6%; morphine 23.2±4.3%, $F_{2,56}$=5.8, p=0.01, one-way ANOVA,

p=0.01 saline vs. cocaine, p=0.04 saline vs. morphine, Bonferroni posttest). Based on these considerations, cell type-specific generation of silent synapses is a bona fide conclusion, at least at a semi-quantitative level.

Excitatory synapses on NAc D1R and D2R MSNs undergo differential molecular and cellular adaptations after exposure to cocaine and differentially contribute to cocaine-induced behaviors[26]. For example, the density of dendritic spines and the frequency of miniature EPSCs are selectively and persistently increased in D1R NAc MSNs after exposure to cocaine[43,44]. Furthermore, accumulation of FosB after cocaine withdrawal is also selectively observed in D1R MSNs, and overexpression of FosB increases the number of immature spines in D1R but not D2R NAc MSNs[13,25,45]. In addition, the ratio of synaptic strength on D1R vs. D2R MSNs is increased in certain excitatory projections to the NAc after exposure to cocaine[46]. These results are in concert with our findings that D1R MSNs are primarily targeted by cocaine for synaptogenesis and strengthening of excitatory synapses. On the other hand, our present results demonstrate a distinct form of silent synapse-based synaptic remodeling selectively in D2R NAcSh MSNs after morphine exposure, which may decrease the overall excitatory drive to these neurons. Consistent with this notion, recent findings show that withdrawal from morphine decreases the frequency, but not the amplitude, of miniature EPSCs in D2R NAc MSNs[47], an effect that can result from synapse elimination. Given that the two subtypes of NAc MSNs often exert antagonistic effects on acute drug-related behaviors—namely activation of D1R MSNs or inhibition of D2R MSNs enhances behavioral responses to drugs of abuse[12,48], the differential effects of cocaine and morphine perceivably produce an equivalent circuitry consequence, a shift in the balance between excitatory inputs to D1R versus D2R NAc MSNs.

In parallel to generation of silent synapses and potential synapse elimination in D2R NAc MSNs, recent results show that exposure to morphine also alters excitatory synapses on D1R MSNs. For example, withdrawal from morphine increases the ratio of AMPAR- to NMDAR-mediated EPSCs in D1R MSNs, suggesting a potentiation of these synapses[47]. These effects are thought to be mediated by synaptic insertion of new, GluA2-lacking AMPARs[47], and are thus unlikely to be prevented by GluA2-interacting peptide GluA2$_{3Y}$. These effects of morphine in D1R MSNs may contribute to the persisting morphine-induced locomotor responses in GluA2$_{3Y}$-adminstered mice (Fig. 7; Supplementary Fig. 2), supporting the notion that a D1R NAc MSN circuit predominates in drug-induced locomotor responses[48].

Using cell type-specific expression of tetanus toxin, recent studies demonstrate that inhibiting the output of D1R, but not D2R, NAc MSNs impairs the acquisition of cocaine- or palatable food-induced CPP as well as acquisition of reward-directed operant tasks[48,49]. Our present results show that preventing silent synapse-based remodeling of a D2R NAc MSN circuit disrupted morphine-induced CPP (Fig. 7), revealing a new role for D2R MSN-specific synaptic remodeling in conditioned drug responses. Silent synapse-based D2R MSN-specific circuit remodeling may contribute to morphine-induced CPP at several levels. First, similar to D1R MSN-oriented effects by cocaine, D2R MSN-selective synaptic weakening by morphine causes the same direction of shift between the excitatory inputs to D1R versus D2R MSNs, and this shift may serve as an essential step for acquiring

conditioned responses. Second, D2R MSN-specific circuit remodeling may also contribute to the retention of acquired CPP. Previous studies demonstrate that a similar morphine procedure induces CPP that persists for >12 weeks[16]. Such long-term CPP-related memories must be retained by mechanisms that are sufficiently rigid and durable to persist despite different forms of memory dissipation processes over time. One consequence of silent synapse-mediated synaptic remodeling is the reduced driving force and thus reduced functional output of D2R NAc MSNs. It is observed that animals with inhibited output of D2R NAc MSNs are rigidly locked to established reward-conditioned responses and resistant to updated conditioning[49]. Thus, silent synapse-mediated weakening of the D2R NAc MSN circuit may contribute to the stabilization of morphine-induced CPP. Third, activation of D2R NAc MSNs induces conditioned place aversion[12,50]. Reduced activity of D2R NAc MSNs after silent synapse-mediated circuitry remodeling may thus also decrease the morphine- or morphine withdrawal-associated anhedonic effects, facilitating CPP acquisition or retention.

The present findings leave unanswered at least three major questions. First, NAc D1R and D2R MSNs receive excitatory projections from several brain regions. Is the cell type-specific generation of silent synapses also projection-specific? Second, does the cell-type specific rule hold after contingent exposure to cocaine and morphine? Third, our present results as well as other published findings support the notion that D1R vs. D2R NAc MSNs play distinct or opposing roles in mediating the relatively acute effects of drugs of abuse. Do D1R and D2R MSNs also play distinct roles after chronic drug exposure and withdrawal and do D1R and D2R MSN circuits coordinate in mediating certain behaviors? Answering these questions may reveal a common circuit-based mechanism underlying shared features of the addictive state.

Online Methods

Animals

Animals were male Sprague-Dawley rats (200–250g; 50–80d old) (Wilmington, MA; Charles River), male B51 wild type, or male Drd1a-tdTomato mice (~25g; 50–80d old) (Bar Harbor, MA; Jackson Laboratory). Rats and mice were singly housed on a regular 12h light/dark cycle (light on at 07:00 AM) with food and water available ad libitum. The animals were used in all experiments in accordance with protocols approved by the Institutional Animal Care and Use Committees at University of Pittsburgh or Mount Sinai School of Medicine.

Repeated systematic injections of saline, cocaine, or morphine

Before drug administration or molecular manipulation, rats or mice were allowed to acclimate to their home cages for >5d. For drug treatment, we used a 5d repeated drug administration procedure[8]. In all electrophysiological and morphological experiments (Figs. 1–6), once per d for 5d, rats or mice were taken out of the home cages at 7–9am for an intraperitoneal (i.p.) injection of either (−)-cocaine HCl (15mg/kg in saline), (−)-morphine sulfate pentahydrate (10mg/kg in saline), or the same volume of saline, and then placed back to the home cage. In behavioral experiments (Fig. 7), subcutaneous (s.c.), rather than i.p.,

injections were used for systematic delivery of morphine, and i.p. injections were used for saline and cocaine. These doses and routes of drug delivery were selected as they produce equivalent degrees of locomotor sensitization and conditioned reward for the two drugs[16, 51]. Animals were randomly selected for each drug treatment. Contextual cues associated with drug injection[52] were intentionally not provided. Cocaine-, morphine-, or saline-treated animals were then used for electrophysiological recordings ~24h following the last injection. For time course studies, animals received 1-, 2-, 3-, or 5d treatment and electrophysiological recordings were taken ~24h following the last injection, In other experiments, rats receiving a 5d daily injection paradigm of morphine or saline were used on withdrawal d7 (Fig. 1). In experiments involving long-term withdrawal (Figs. 2, 3), animals were killed for imaging or electrophysiological studies 21–28d after the last drug injection.

Intravenous tail vein injections

Rats or mice were weighed before injections to prevent an administered volume greater than 1% of the animal's body weight. Prior to each injection of peptides (scrambled TAT-conjugated GluA2$_{3A}$ peptide, YGRKKRRQRRR-VYKYGGYNE; or TAT-conjugated GluA2$_{3Y}$, YGRKKRRQRRR-YKEGYNVYG; 1.5nm/g), the rats were placed on a heating pad for 5–10min. Rats were lightly anesthetized with isoflurane (inhalation), placed on a heating pad, and positioned on their side. The tail was cleaned with alcohol. The lateral tail vein was identified and the peptides were injected 15min prior to injection of cocaine or morphine to allow peptide and drug to reach the brain at approximately the same time[21].

Preparation of NAc acute slices

For acute slices, rats or mice were decapitated following isoflurane anesthesia. Coronal slices (250μm) containing the NAc were prepared on a VT1200S vibratome (Leica, Germany) in 4°C cutting solution containing (in mM): 135 N-methyl-D-glutamine, 1 KCl, 1.2 KH$_2$PO$_4$, 0.5 CaCl$_2$, 1.5 MgCl$_2$, 20 choline-HCO$_3$, and 11 glucose, saturated with 95%O$_2$/5%CO$_2$, pH adjusted to 7.4 with HCl. Osmolality adjusted to 305. Slices were incubated in artificial cerebrospinal fluid (aCSF) containing (in mM): 119 NaCl, 2.5 KCl, 2.5 CaCl$_2$, 1.3 MgCl$_2$, 1 NaH$_2$PO$_4$, 26.2 NaHCO$_3$, and 11 glucose with the osmolality adjusted to 280–290. aCSF was saturated with 95% O$_2$ / 5% CO$_2$ at 37° C for 30 min and then allowed to recover for >30min at room temperature before experimentation.

Electrophysiological recordings

Whole-cell recording—All recordings were made from MSNs located in the ventral-medial NAcSh. During recordings, slices were superfused with aCSF, heated to 30–32°C by passing the solution through a feedback-controlled in-line heater (Warner, CT) before entering the recording chamber. To measure minimal stimulation-evoked responses, the coefficient of variance, or the ratio of EPSC amplitude between D1R and D2R MSNs, electrodes (2–5 MΩ) were filled with a cesium-based internal solution (in mM: 135 CsMeSO3, 5 CsCl, 5 TEA-Cl, 0.4 EGTA (Cs), 20 HEPES, 2.5 Mg-ATP, 0.25 Na-GTP, 1 QX-314 (Br), pH 7.3). Picrotoxin (100μM) was included in the aCSF during recordings to inhibit GABA$_A$ receptor-mediated currents. Presynaptic afferents were stimulated by a constant-current isolated stimulator (Digitimer, UK), using a monopolar electrode (glass

pipette filled with aCSF). Series resistance was 9–20 M, uncompensated, and monitored continuously during recording. Cells with a change in series resistance beyond 15% were not accepted for data analysis. Synaptic currents were recorded with a MultiClamp 700B amplifier, filtered at 2.6–3kHz, amplified 5 times, and then digitized at 20kHz.

Silent synapse recordings and analysis—Neurons in the NAcSh were randomly selected for recording. Minimal stimulation experiments were performed as previously reported[8, 18, 53]. After obtaining a small (<50 pA) EPSC at −70 mV, the stimulation intensity was reduced in small increments to the point that failures vs. successes of synaptically evoked events (EPSCs) could be clearly distinguished visually (Fig. S2). Stimulation intensity and frequency were then kept constant for the rest of the experiment. The amplitude of both AMPAR and NMDAR ESPCs resulting from single vesicle release is relatively large (e.g., ~15 pA for AMPAR mEPSCs)[8], which facilitates the judgment of success vs. failures of EPSCs; therefore, they were defined visually. For each cell, 50–100 traces were recorded at −70 mV, and 50–100 traces were recorded at +50 mV. Recordings were then repeated at −70 mV and +50 mV for another round or two. Each cell was recorded >2 rounds. Only cells with relatively constant failure rates (changes <10%) between rounds were included for calculation of % silent synapses. We visually detected failures vs. successes at each holding potential over 50–100 trials to calculate the failure rate, as described previously[8, 18, 53]. We performed this analysis in a blind manner such that a small number of ambiguous responses were categorized in a fully unbiased way. We made two theoretical assumptions: 1) the presynaptic release sites are independent, and 2) release probability across all synapses, including silent synapses, is identical. Thus, percent silent synapses were calculated using the equation: $1-Ln(F_{-70})/Ln(F_{+50})$, in which F_{-70} was the failure rate at −70 mV and F_{+50} was the failure rate at +50 mV, as rationalized previously[18]. In the cases in which these two theoretical assumptions are not true, the above equation was still used, as the results were still valid in predicting the changes of silent synapses qualitatively as previously rationalized[5, 10]. The amplitude of an EPSC was determined as the mean value of the EPSC over a 1ms time window around the peak, which was typically 3–4ms after the stimulation artifact (Supplementary Fig. 2a,b). It is worth noting that the amplitudes and the trails of amplitudes of EPSCs are presented to illustrate the time courses of successes and failures over the experiments. To assess % silent synapses, only the rates of failures vs. successes, not the absolute values of the amplitudes, were used. At +50 mV, successful synaptic responses were conceivably mediated by both AMPARs and NMDARs, and inhibiting AMPARs by NBQX (5 μM) modestly reduced the amplitudes of EPSCs (Supplementary Fig. 2c–f). Despite the effects of NBQX on the amplitudes, the failure rate of synaptic responses at +50 mV was not altered during AMPAR inhibition (Supplementary Fig. 2g). Thus, in the minimal stimulation assay assessing % silent synapses, the results will not be affected whether the synaptic responses +50 mV are mediated by NMDARs alone or by both AMPARs and NMDARs.

Imaging dendritic spines

Dendritic spines of NAcSh MSNs were labeled and imaged as described previously[11, 22]. Briefly, rats or mice were perfused transcardially (20ml/min) with 0.1M sodium phosphate buffer (PB), followed by 200ml of 1.5% paraformaldehyde (PFA) in 0.1M PB. The use of

1.5% rather than the traditional 4% PFA was critical in obtaining maximal dye filling of small diameter spines. Brains were removed and postfixed in the same fixative for 1h at room temperature before coronal slices of 100μm thickness were prepared. The slices were collected in PB-saline and mounted before DiI labeling. DiI fine crystals (Invitrogen) were delivered under a dissecting microscope onto the surface of slices using a fine brush, controlled by a micromanipulator. DiI was allowed to diffuse in PBS for 48h at 4°C, and then labeled sections were fixed in 4% PFA at room temperature for 1h. After brief wash in PBS, tissues were mounted in aqueous medium prolong (Invitrogen).

An Olympus confocal microscope was used to image the labeled sections. DiI was excited using the Helium/Neon 559nm laser line. The entire profile of each DiI-positive neuron to be quantified was acquired using a 60x oil-immersion objective. After the neuron was scanned and confirmed as an NAcSh MSN, its dendrites were focused using a 60x oil-immersion objective and scanned at 0.44μm intervals along the z-axis for a maximum of 200 planes; the final image of each dendrite was obtained by stacking all planes. Analyses were performed on two-dimensional projection images using the software ImageJ (NIH). Based on previous results[2, 3], secondary dendrites were preferentially sampled. For each neuron, one or two dendrites of 20μm in length were analyzed. For each group, 5–10 neurons/animal were analyzed. We operationally divided the spines into four categories[11, 43]: i) mushroom-like spines were dendritic protrusions with a head diameter >0.5μm or 2x the neck diameter; ii) stubby spines were dendritic protrusions with no discernible head and with a length 0.5μm; iii) filopodia-like spines were dendritic protrusions with no discernible head and with a length > 0.5μm; and iv) long-thin spines were dendritic protrusions with a head diameter < 2x the neck diameter. The density of long-thin spines can also be obtained by subtracting mushroom, stubby, and filopodia spines from the total spines.

Drug-induced Locomotor responses

During light cycles, mice were allowed to habituate to the commercially available locomotor chamber (18.0″ L x 9.5″ W x 12.0″ H) (Camden Instruments, Loughborough, England) 1h/d for 2d before the d0 injection. Locomotor activity was measured using infrared photobeams for 1h and the average distance traveled (m) over 4 15-min bins was presented[54]. Mice were immediately returned to their home cage after each session. 21d after the 5d procedure, mice received challenge drug injections with ascending doses. Cocaine and morphine was delivered through i.p. and s.c. injections, respectively. For experiments involving peptides, $GluA_23Y$ or scrambled peptide was injected into the tail vein ~20min before saline, cocaine or morphine injection.

Conditioned place preference

Chambers—The mouse CPP chamber (Med Associates, St. Albans, VT) was consisted of 3 compartments, separated by manual guillotine doors. The 3 compartments had distinct characteristics: the center compartment ($2.85″ \times 5″ \times 5″$) had gray walls and floor, the two choice compartments ($6.6″ \times 5″ \times 5″$) differed in wall color (white vs. black with white stripes) and floor texture (stainless steel mesh floor vs. stainless steel grid). After each test, compartments were thoroughly cleaned with a scent-free soap solution. Each compartment was illuminated with a dim light situated in the laminate top. Mouse locations were

identified by automated data collection software (Med Associates) using infrared photobeam strips that recorded the time spent in each compartment.

Preconditioning—During light cycles, mice were habituated to the testing room for 30min before each session. Mice were then placed in the center compartment with free access to all three compartments for 20min. Time spent (seconds) in each compartment was recorded.

Conditioning—24 h after preconditioning, mice received a 5d conditioning training. Drug-paired compartments were randomly assigned[55]. For test involving peptides, mice received bilateral intra-NAcSh (AP, +1.75; ML, ±0.6; DV, −3.5mm) infusion of GluA2$_{3Y}$ or scrambled peptide (30pmol in 1μl) through preinstalled guide cannula. Mice were then habituated to the testing room for 30min, before conditioning experiments. During conditioning, mice received an injection of saline or cocaine (15mg/kg) or morphine (10mg/kg) and were placed into one compartment for 40min in the morning and to the opposite compartment in the afternoon[56]. Morning and afternoon sessions were separated by 6h.

Post-conditioning—24h and 21d after the last conditioning day (d6 and d28), mice were habituated to the testing room for 30min and then placed in the center compartment, where they were allowed to move freely for 20min. CPP scores were calculated as time spent in the drug-paired side minus the time spent on the same side during the preconditioning day[57].

Drugs

Picrotoxin was purchased from Sigma Aldrich (St. Louis, MO). (−)-Morphine sulfate pentahydrate and (−)cocaine HCl was provided by the National Institute on Drug Abuse Drug Supply Program.

Data acquisition and statistics

In electrophysiology experiments, we used 152 rats and 70 D1-tomato mice. In locomotor tests, we used a total of 136 C57bl/6 mice, with 7 of them excluded before data collection due to death during drug withdrawal. In CPP tests, we used 70 mice, among which 13 were removed from data analysis due to inaccurate cannula placement or strong preference to one chamber before conditioning. In imaging experiments, we used 113 rats with 9 of them excluded from data collection due to death, and 119 C57bl/6 mice, with 12 of them excluded from data collection due to death.

All results are shown as mean±SEM. Each experiment was replicated in 3–12 animals. The data collection was randomized. Data were obtained and analyzed by experimenters who did not know the types of treatments of the animals. No data points were excluded unless specified, and the only exclusion standard is the health condition of the animal. Data from the repeated experiments for the same sub-study were pooled together for statistics. Technical replicates were utilized for some of the key experiments. Sample size for each experiment was determined either based on our previous experience with similar

experiments or those that have been routinely used in similar studies published in this journal (Ref #5,9). Sample size was presented as n/m, where "n" refers to the number of cells, cell pairs, or dendrites examined, and "m" refers to the number of animals. In electrophysiological experiments, 1–4 recordings were performed using slices from a single animal. In morphological experiments, 3–10 dendrites were assessed from a single animal. Animal-based statistics were performed and reported for all results. In electrophysiological and morphological experiments, we used the averaged value of a parameter from all cells/dendrites from an animal to represent the parameter of this animal. Normal distribution was assumed for all statistics but this was not formally tested. Variance was estimated for most major results and no significant difference was found between control and manipulation groups. Statistical significance was assessed using the *t*-test, or one- or two-way ANOVA as specified. Two-tail tests were performed for all studies. A supplementary methods checklist of this manuscript is available on line.

Supplementary Material

Refer to Web version on PubMed Central for supplementary material.

Acknowledgments

References

1. Wolf ME. The Bermuda Triangle of cocaine-induced neuroadaptations. Trends Neurosci. 2010; 33:391–398. [PubMed: 20655604]

2. Robinson TE, Gorny G, Savage VR, Kolb B. Widespread but regionally specific effects of experimenter- versus self-administered morphine on dendritic spines in the nucleus accumbens, hippocampus, and neocortex of adult rats. Synapse. 2002; 46:271–279. [PubMed: 12373743]

3. Robinson TE, Kolb B. Alterations in the morphology of dendrites and dendritic spines in the nucleus accumbens and prefrontal cortex following repeated treatment with amphetamine or cocaine. Eur J Neurosci. 1999; 11:1598–1604. [PubMed: 10215912]

4. Dong Y, Nestler EJ. The neural rejuvenation hypothesis of cocaine addiction. Trends in pharmacological sciences. 2014; 35:374–383. [PubMed: 24958329]

5. Huang YH, Schluter OM, Dong Y. Silent Synapses Speak Up: Updates of the Neural Rejuvenation Hypothesis of Drug Addiction. Neuroscientist. 2015

6. Kerchner GA, Nicoll RA. Silent synapses and the emergence of a postsynaptic mechanism for LTP. Nat Rev Neurosci. 2008; 9:813–825. [PubMed: 18854855]

7. Hanse E, Seth H, Riebe I. AMPA-silent synapses in brain development and pathology. Nat Rev Neurosci. 2013; 14:839–850. [PubMed: 24201185]

8. Huang YH, et al. In vivo cocaine experience generates silent synapses. Neuron. 2009; 63:40–47. [PubMed: 19607791]

9. Lee BR, et al. Maturation of silent synapses in amygdala-accumbens projection contributes to incubation of cocaine craving. Nature neuroscience. 2013; 16:1644–1651. [PubMed: 24077564]

10. Ma YY, et al. Bidirectional modulation of incubation of cocaine craving by silent synapse-based remodeling of prefrontal cortex to accumbens projections. Neuron. 2014; 83:1453–1467. [PubMed: 25199705]

11. Brown TE, et al. A silent synapse-based mechanism for cocaine-induced locomotor sensitization. J Neurosci. 2011; 31:8163–8174. [PubMed: 21632938]

12. Lobo MK, et al. Cell type-specific loss of BDNF signaling mimics optogenetic control of cocaine reward. Science. 2010; 330:385–390. [PubMed: 20947769]

13. Lobo MK, Nestler EJ. The striatal balancing act in drug addiction: distinct roles of direct and indirect pathway medium spiny neurons. Front Neuroanat. 2011; 5:41. [PubMed: 21811439]

14. Kravitz AV, Tye LD, Kreitzer AC. Distinct roles for direct and indirect pathway striatal neurons in reinforcement. Nature neuroscience. 2012; 15:816–818. [PubMed: 22544310]

15. Spanagel R, et al. Acamprosate suppresses the expression of morphine-induced sensitization in rats but does not affect heroin self-administration or relapse induced by heroin or stress. Psychopharmacology (Berl). 1998; 139:391–401. [PubMed: 9809860]

16. Mueller D, Perdikaris D, Stewart J. Persistence and drug-induced reinstatement of a morphine-induced conditioned place preference. Behav Brain Res. 2002; 136:389–397. [PubMed: 12429400]

17. Kullmann DM. Amplitude fluctuations of dual-component EPSCs in hippocampal pyramidal cells: implications for long-term potentiation. Neuron. 1994; 12:1111–1120. [PubMed: 7910467]

18. Liao D, Hessler NA, Malinow R. Activation of postsynaptically silent synapses during pairing-induced LTP in CA1 region of hippocampal slice. Nature. 1995; 375:400–404. [PubMed: 7760933]

19. Boudreau AC, Wolf ME. Behavioral sensitization to cocaine is associated with increased AMPA receptor surface expression in the nucleus accumbens. J Neurosci. 2005; 25:9144–9151. [PubMed: 16207873]

20. Ahmadian G, et al. Tyrosine phosphorylation of GluR2 is required for insulin-stimulated AMPA receptor endocytosis and LTD. EMBO J. 2004; 23:1040–1050. [PubMed: 14976558]

21. Brebner K, et al. Nucleus accumbens long-term depression and the expression of behavioral sensitization. Science. 2005; 310:1340–1343. [PubMed: 16311338]

22. Shen HW, et al. Altered dendritic spine plasticity in cocaine-withdrawn rats. J Neurosci. 2009; 29:2876–2884. [PubMed: 19261883]

23. Holtmaat A, Svoboda K. Experience-dependent structural synaptic plasticity in the mammalian brain. Nat Rev Neurosci. 2009; 10:647–658. [PubMed: 19693029]

24. Shuen JA, Chen M, Gloss B, Calakos N. Drd1a-tdTomato BAC transgenic mice for simultaneous visualization of medium spiny neurons in the direct and indirect pathways of the basal ganglia. J Neurosci. 2008; 28:2681–2685. [PubMed: 18337395]

25. Lobo MK, et al. DeltaFosB induction in striatal medium spiny neuron subtypes in response to chronic pharmacological, emotional, and optogenetic stimuli. J Neurosci. 2013; 33:18381–18395. [PubMed: 24259563]

26. Smith RJ, Lobo MK, Spencer S, Kalivas PW. Cocaine-induced adaptations in D1 and D2 accumbens projection neurons (a dichotomy not necessarily synonymous with direct and indirect pathways). Curr Opin Neurobiol. 2013; 23:546–552. [PubMed: 23428656]

27. Kam AY, Liao D, Loh HH, Law PY. Morphine induces AMPA receptor internalization in primary hippocampal neurons via calcineurin-dependent dephosphorylation of GluR1 subunits. J Neurosci. 2010; 30:15304–15316. [PubMed: 21068335]

28. Koya E, et al. Silent synapses in selectively activated nucleus accumbens neurons following cocaine sensitization. Nature neuroscience. 2012; 15:1556–1562. [PubMed: 23023294]

29. Arellano JI, Espinosa A, Fairen A, Yuste R, DeFelipe J. Non-synaptic dendritic spines in neocortex. Neuroscience. 2007; 145:464–469. [PubMed: 17240073]

30. Grutzendler J, Kasthuri N, Gan WB. Long-term dendritic spine stability in the adult cortex. Nature. 2002; 420:812–816. [PubMed: 12490949]

31. Zuo Y, Yang G, Kwon E, Gan WB. Long-term sensory deprivation prevents dendritic spine loss in primary somatosensory cortex. Nature. 2005; 436:261–265. [PubMed: 16015331]

32. Khibnik LA, et al. Stress and Cocaine Trigger Divergent and Cell Type-Specific Regulation of Synaptic Transmission at Single Spines in Nucleus Accumbens. Biol Psychiatry. 2015

33. Fiala JC, Feinberg M, Popov V, Harris KM. Synaptogenesis via dendritic filopodia in developing hippocampal area CA1. J Neurosci. 1998; 18:8900–8911. [PubMed: 9786995]

34. Knott GW, Holtmaat A, Wilbrecht L, Welker E, Svoboda K. Spine growth precedes synapse formation in the adult neocortex in vivo. Nature neuroscience. 2006; 9:1117–1124. [PubMed: 16892056]

35. Trachtenberg JT, et al. Long-term in vivo imaging of experience-dependent synaptic plasticity in adult cortex. Nature. 2002; 420:788–794. [PubMed: 12490942]

36. Takumi Y, Ramirez-Leon V, Laake P, Rinvik E, Ottersen OP. Different modes of expression of AMPA and NMDA receptors in hippocampal synapses. Nature neuroscience. 1999; 2:618–624. [PubMed: 10409387]

37. Matsuzaki M, et al. Dendritic spine geometry is critical for AMPA receptor expression in hippocampal CA1 pyramidal neurons. Nature neuroscience. 2001; 4:1086–1092. [PubMed: 11687814]

38. Racca C, Stephenson FA, Streit P, Roberts JD, Somogyi P. NMDA receptor content of synapses in stratum radiatum of the hippocampal CA1 area. J Neurosci. 2000; 20:2512–2522. [PubMed: 10729331]

39. Nimchinsky EA, Yasuda R, Oertner TG, Svoboda K. The number of glutamate receptors opened by synaptic stimulation in single hippocampal spines. J Neurosci. 2004; 24:2054–2064. [PubMed: 14985448]

40. Holtmaat AJ, et al. Transient and persistent dendritic spines in the neocortex in vivo. Neuron. 2005; 45:279–291. [PubMed: 15664179]

41. Zito K, Scheuss V, Knott G, Hill T, Svoboda K. Rapid functional maturation of nascent dendritic spines. Neuron. 2009; 61:247–258. [PubMed: 19186167]

42. Gerfen CR, et al. D1 and D2 dopamine receptor-regulated gene expression of striatonigral and striatopallidal neurons. Science. 1990; 250:1429–1432. [PubMed: 2147780]

43. Lee KW, et al. Cocaine-induced dendritic spine formation in D1 and D2 dopamine receptor-containing medium spiny neurons in nucleus accumbens. Proc Natl Acad Sci U S A. 2006; 103:3399–3404. [PubMed: 16492766]

44. Kim J, Park BH, Lee JH, Park SK, Kim JH. Cell type-specific alterations in the nucleus accumbens by repeated exposures to cocaine. Biol Psychiatry. 2011; 69:1026–1034. [PubMed: 21377654]

45. Grueter BA, Robison AJ, Neve RL, Nestler EJ, Malenka RC. FosB differentially modulates nucleus accumbens direct and indirect pathway function. Proc Natl Acad Sci U S A. 2013; 110:1923–1928. [PubMed: 23319622]

46. MacAskill AF, Cassel JM, Carter AG. Cocaine exposure reorganizes cell type- and input-specific connectivity in the nucleus accumbens. Nature neuroscience. 2014; 17:1198–1207. [PubMed: 25108911]

47. Hearing MC, et al. Reversal of morphine-induced cell-type-specific synaptic plasticity in the nucleus accumbens shell blocks reinstatement. Proc Natl Acad Sci U S A. 2016; 113:757–762. [PubMed: 26739562]

48. Hikida T, Kimura K, Wada N, Funabiki K, Nakanishi S. Distinct roles of synaptic transmission in direct and indirect striatal pathways to reward and aversive behavior. Neuron. 2010; 66:896–907. [PubMed: 20620875]

49. Yawata S, Yamaguchi T, Danjo T, Hikida T, Nakanishi S. Pathway-specific control of reward learning and its flexibility via selective dopamine receptors in the nucleus accumbens. Proc Natl Acad Sci U S A. 2012; 109:12764–12769. [PubMed: 22802650]

50. Yamaguchi T, Danjo T, Pastan I, Hikida T, Nakanishi S. Distinct roles of segregated transmission of the septo-habenular pathway in anxiety and fear. Neuron. 2013; 78:537–544. [PubMed: 23602500]

51. Stinus L, Cador M, Zorrilla EP, Koob GF. Buprenorphine and a CRF1 antagonist block the acquisition of opiate withdrawal-induced conditioned place aversion in rats. Neuropsychopharmacology. 2005; 30:90–98. [PubMed: 15138444]

52. Badiani A, Camp DM, Robinson TE. Enduring enhancement of amphetamine sensitization by drug-associated environmental stimuli. J Pharmacol Exp Ther. 1997; 282:787–794. [PubMed: 9262342]

53. Isaac JT, Nicoll RA, Malenka RC. Evidence for silent synapses: implications for the expression of LTP. Neuron. 1995; 15:427–434. [PubMed: 7646894]

54. Schoenbaum G, Saddoris MP, Ramus SJ, Shaham Y, Setlow B. Cocaine-experienced rats exhibit learning deficits in a task sensitive to orbitofrontal cortex lesions. Eur J Neurosci. 2004; 19:1997–2002. [PubMed: 15078575]

55. Blander A, Hunt T, Blair R, Amit Z. Conditioned place preference: an evaluation of morphine's positive reinforcing properties. Psychopharmacology (Berl). 1984; 84:124–127. [PubMed: 6436880]

56. Koo JW, et al. BDNF is a negative modulator of morphine action. Science. 2012; 338:124–128. [PubMed: 23042896]

57. Bohn LM, et al. Enhanced rewarding properties of morphine, but not cocaine, in beta(arrestin)-2 knock-out mice. J Neurosci. 2003; 23:10265–10273. [PubMed: 14614085]
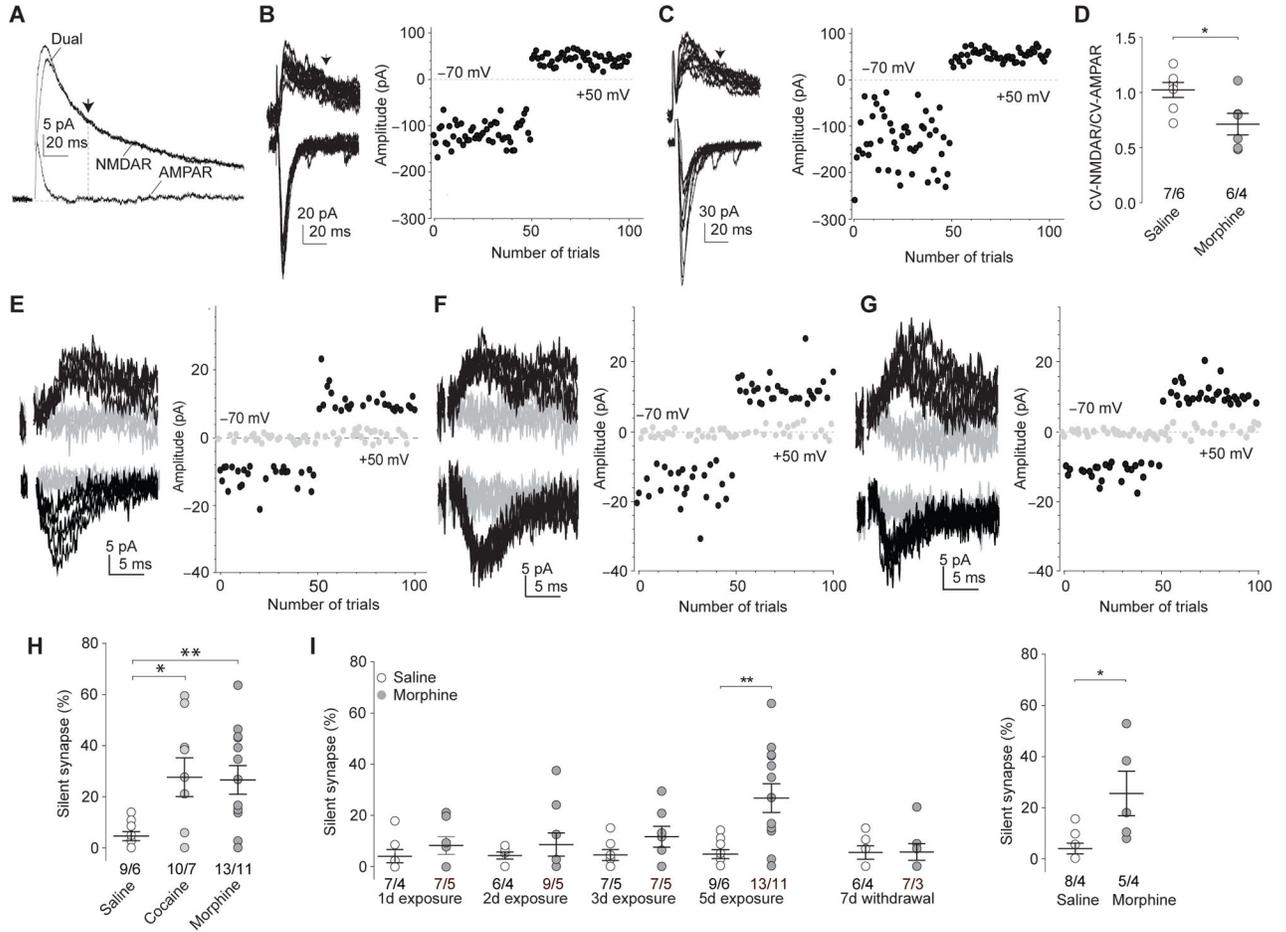
Figure 1. Exposure to morphine generates silent synapses in NAc MSNs

a Example traces (n=13 cells) showing pharmacological separation of AMPAR and NMDAR EPSCs. At 35ms (arrow), the amplitude of dual-component EPSCs was primarily attributable to NMDAR-mediated current. **b,c** Examples and plots of AMPAR (at −70mV) and NMDAR (at +50mV) EPSCs from saline- (n=7/6 cells/rats; **b**) and morphine-exposed (n=6/4 cells/rats; **c**) rats after 1d withdrawal for CV assay. **d** Summary showing a significantly decreased CV-NMDAR/CV-AMPAR ratio in NAcSh MSNs in morphine-exposed rats (t_{11}=2.67, p=0.02, t-test). **e–g** Example EPSCs elicited by minimal stimulations at +50 and −70mV and their trial plots from saline- (n=9/6 cells/rats; **e**), cocaine- (n=10/7 cells/rats; **f**), and morphine-exposed (n=13/11 cells/rats; **g**) rats. **h** Summary showing increased % silent synapses in NAcSh MSNs after 1d withdrawal from cocaine or morphine ($F_{2,28}$=4.85, p=0.02, one-way ANOVA with Bonferroni posttest). **i** *Left*: Summary showing that silent synapses were gradually generated during exposure to morphine and declined after withdrawal (5d data taken from **h**). Data in A-L were collected when rats were ~50d old. *Right*: Summary showing morphine-induced generation of silent synapses in 70–80d old rats (t_{11}=3.00, p=0.01, t-test). Error bar=s.e.m., *p<0.05, and **p<0.01.
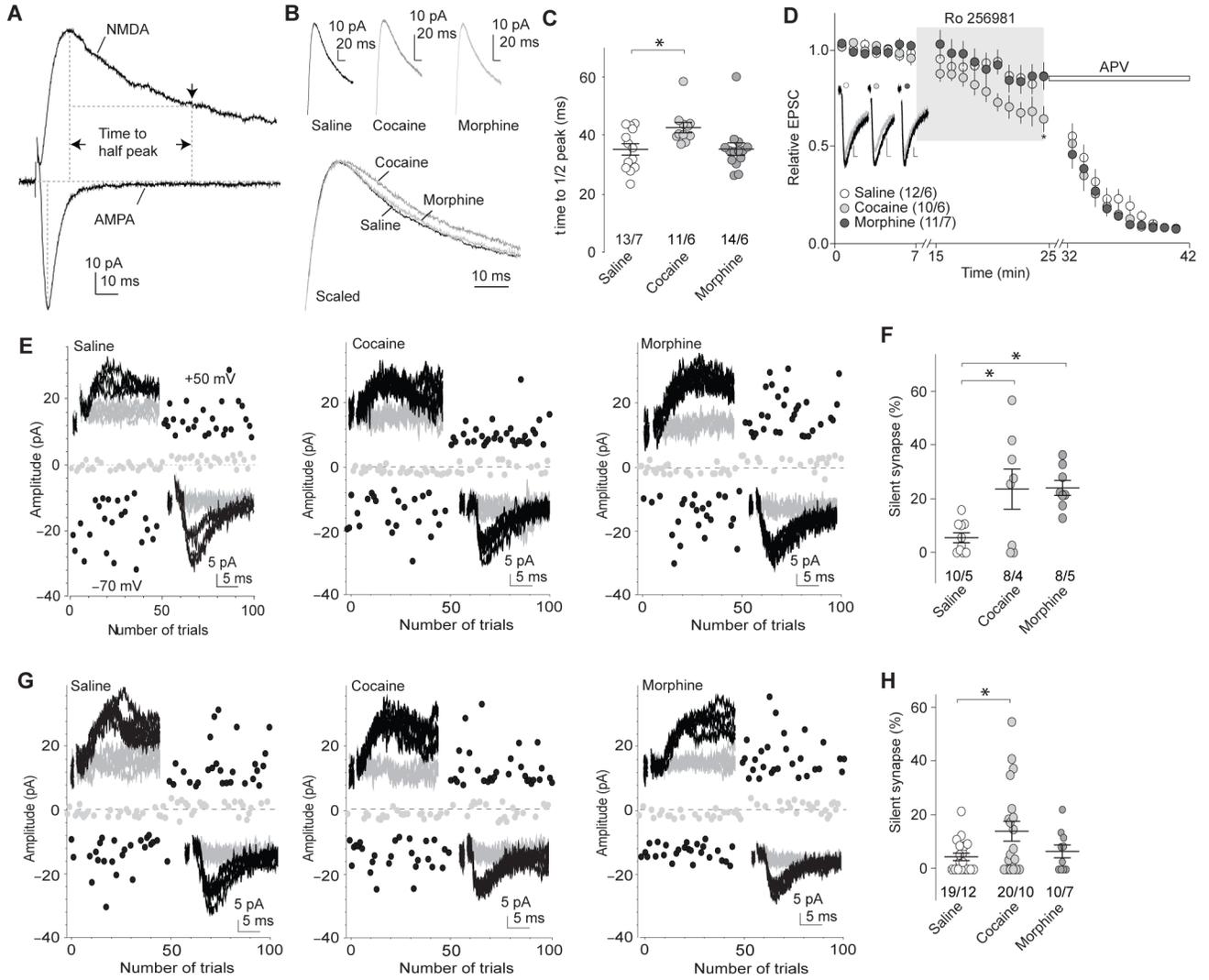
Figure 2. Morphine-induced generation of silent synapses is mediated by AMPAR internalization
a Example traces (n=38 cells) showing that the decay kinetics of NMDAR EPSCs was measured by the half-decay time, the time elapsed from the peak amplitude to half peak amplitude. **b** Example NMDAR EPSCs in NAcSh MSNs 1d after saline (n=13/7 cells/rats), cocaine (n=11/6 cells/rats), or morphine (n=14/6 cells/rats) administration. **c** Summary showing that exposure to cocaine, but not morphine, prolonged the decay kinetics of NMDAR EPSCs ($F_{2,35}$=4.25, p=0.02, one-way ANOVA with Bonferroni posttest). **d** Example traces and summary showing that Ro256981 (200nM) inhibited NMDAR EPSCs in NAcSh MSNs greater in cocaine-exposed rats (n=10/6 cells/rats) than in saline (n=12/6 cells/rats)- or morphine (n=11/7 cells/rats)-exposed rats ($F_{2,810}$=15.71, p=0.00, two-way ANOVA with Bonferroni posttest). Following Ro256981, APV (50μM) was applied. Calibration bars: 10ms, 5pA. **e** Example EPSCs evoked by minimal stimulation and their trial plots in NAcSh MSNs from rats 1d after 5d co-administration of GluA2 scrambled peptide with saline (n=10/5 cells/rats), cocaine (n=8/4 cells/rats), or morphine (n=8/5 cells/rats). **f** Summary showing that co-administration of scrambled peptide did not affect

cocaine- or morphine-induced generation of silent synapses ($F_{2,23}$=6.15, p=0.01, one-way ANOVA with Bonferroni posttest). **g** Example EPSCs evoked by minimal stimulation and their trial plots in NAcSh MSNs from rats 1d after 5d co-administration of GluA2$_{3Y}$ with saline (n=19/12 cells/rats), cocaine (n=20/10 cells/rats), or morphine (n=10/7 cells/rats). **h** Summary showing that co-administration of GluA2$_{3Y}$ prevented morphine-, but not cocaine-induced generation of silent synapses ($F_{2,46}$=3.44, p=0.04, one-way ANOVA with Bonferroni posttest). Error bar=s.e.m., *p<0.05, and **p<0.01.
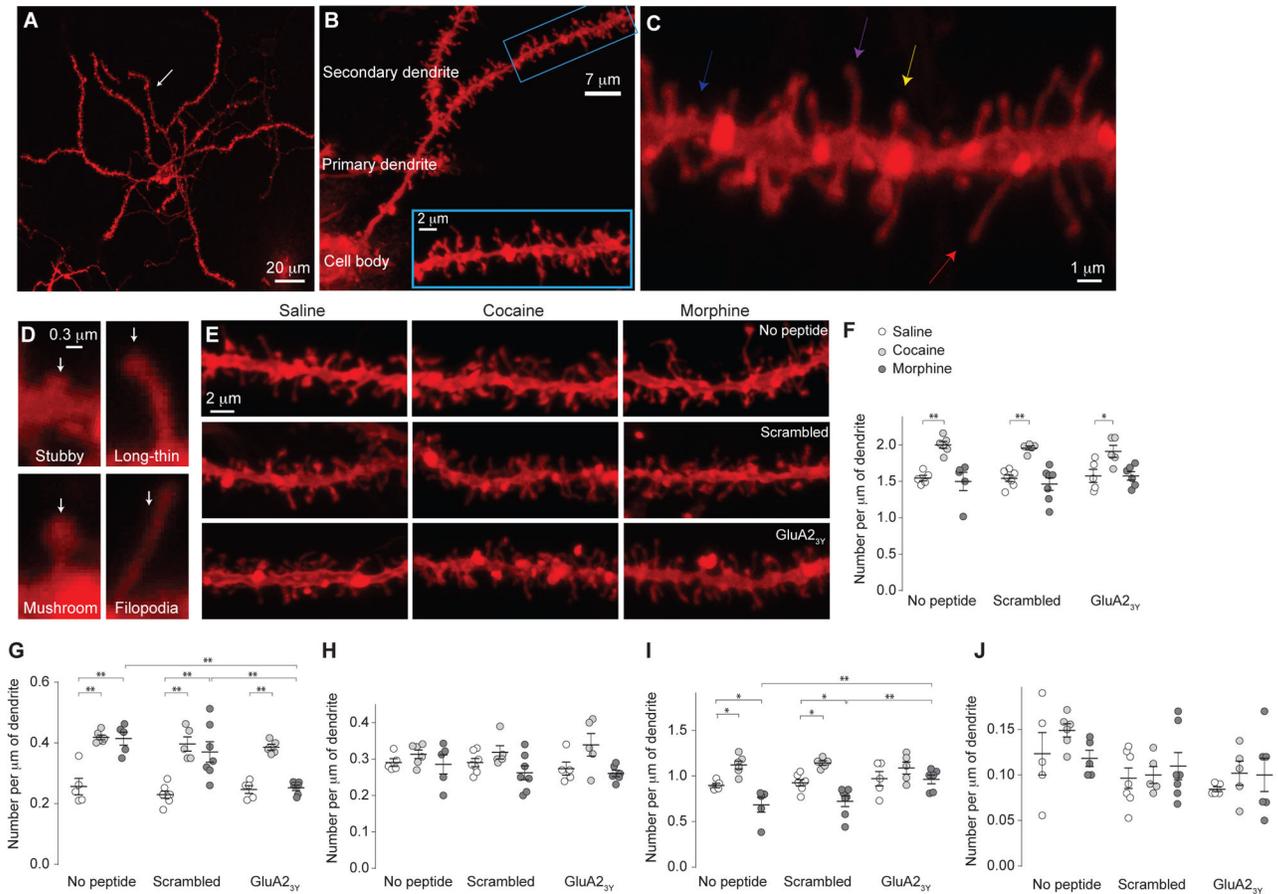
Figure 3. Alterations in spine morphology of rat NAc MSNs 1d after morphine or cocaine administration

a Example image (n=12/6 slices/rats) showing a NAcSh MSN labeled with DiI. Arrow indicates a secondary dendrite. **b** Example images (n=12/6 slices/rats) showing that spines located on secondary dendrites were sampled for spine density analysis. **c,d** Examples of different spine types (n=12/6 slices/rats) along a dendrite (**c**) or individually presented (**d**). Blue, magenta, yellow and red arrows indicate stubby, long-thin, mushroom-like, and filopodia-like spines, respectively. **e** Example images from saline (n=17 rats)-, cocaine (n=16 rats)-, or morphine (n=18 rats)-exposed rats without co-administration of peptides, with co-administration of scrambled peptide, or with co-administration of GluA2$_{3Y}$. **f** Summary showing that total spine density was selectively increased in cocaine-exposed rats, and co-administration of GluA2$_{3Y}$ did not alter this effect ($F_{2,42}$=34.62, p=0.00). **g** Summary showing that density of filopodia-like spines was increased in cocaine- and morphine-exposed rats; co-administration of GluA2$_{3Y}$ prevented morphine-, but not cocaine-, induced increases in filopodia-like spines ($F_{2,42}$=44.91, p=0.00). **h** Summary showing that density of mushroom-like spines was not affected 1d after cocaine or morphine administration ($F_{2,42}$=7.22, p=0.00). **i** Summary showing that density of long-thin spines was increased in cocaine-exposed rats, but decreased in morphine-exposed rats, and these effects were prevented by co-administration of GluA2$_{3Y}$ ($F_{2,42}$=27.56, p=0.00). **j** Summary showing that density of stubby spines was not changed by exposure to cocaine or morphine, and was not

affected by co-administration of GluA2$_{3Y}$ ($F_{2,42}$=0.97, p=0.39). Two-way ANOVA with Bonferroni posttest was used in all above statistics. Error bar=s.e.m., *p<0.05, and **p<0.01.
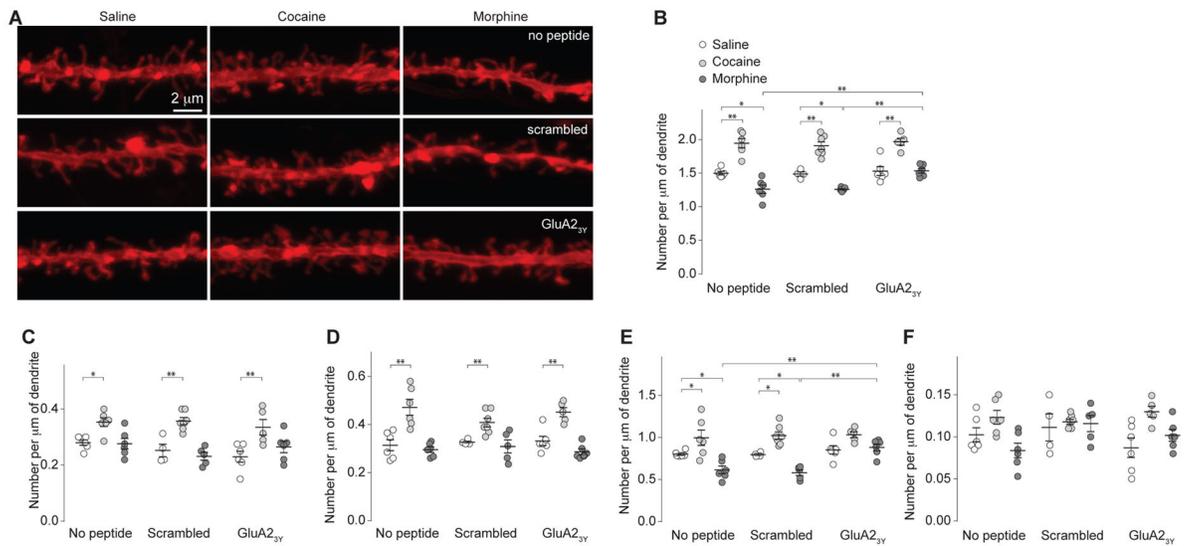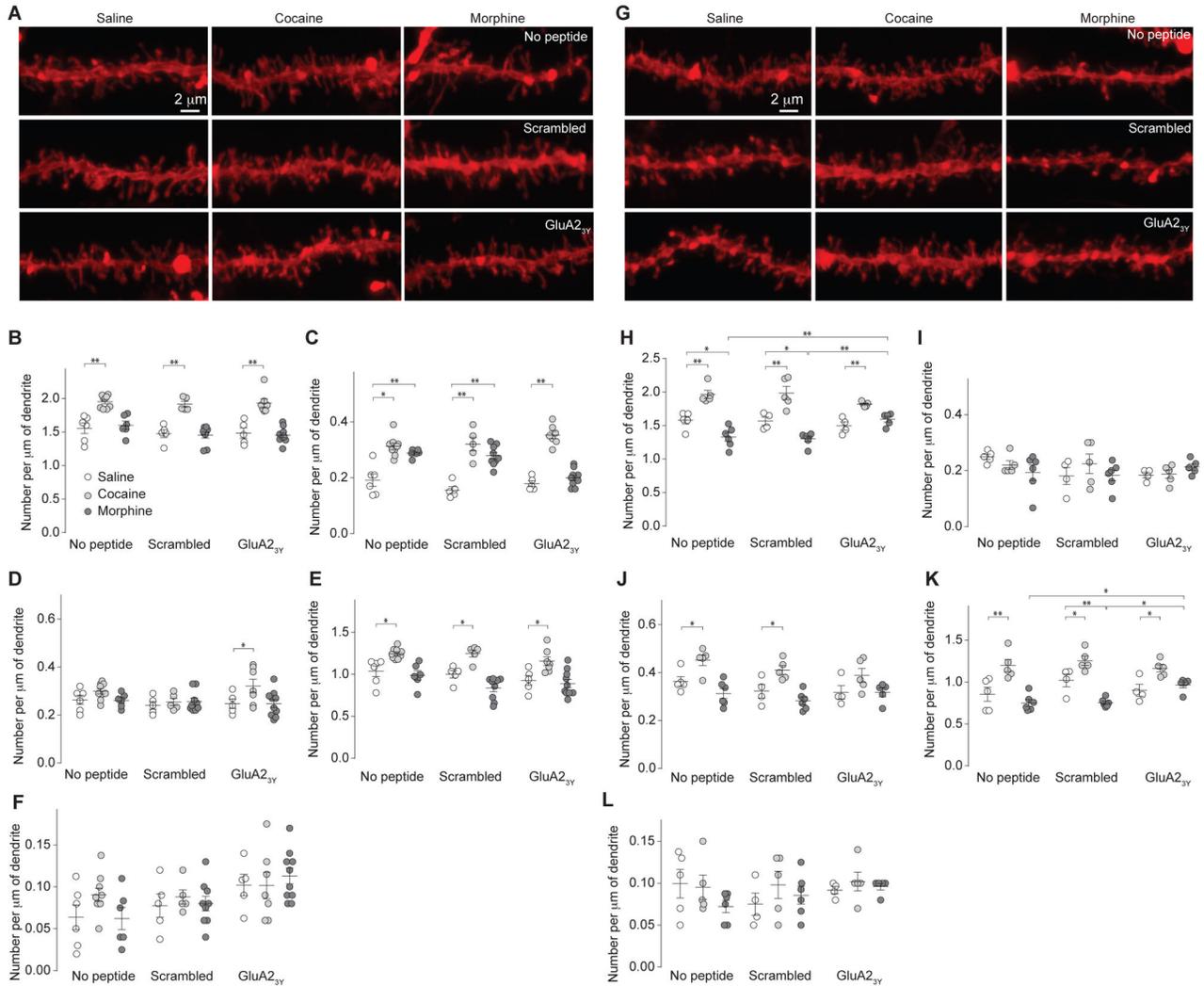
Figure 4. Alterations in spine morphology of rat NAc MSNs 21d after morphine or cocaine administration

All experiments below were performed in rats 21d after the 5d drug procedure. **a** Example images of dendrites in NAcSh slices from saline (n=16 rats)-, cocaine (n=18 rats)-, or morphine (n=17 rats)-exposed rats with or without co-administration of peptides. **b** Summary showing that total spine density was increased in cocaine-exposed rats but decreased in morphine-exposed rats. Co-administration of GluA2$_{3Y}$ selectively prevented morphine-induced decreases in total spines with no effect on cocaine-induced increase in total spines ($F_{2,42}$=100.4, p=0.00, two-way ANOVA with Bonferroni posttest). **c** Summary showing that density of filopodia-like spines was increased in cocaine-exposed rats, and this increased was not affected by co-administration of GluA2 peptides ($F_{2,42}$=25.96, p=0.00, two-way ANOVA with Bonferroni posttest). **d** Summary showing that density of mushroom-like spines was increased in cocaine-exposed rats, and this increase was not affected by co-administration of GluA2 peptides ($F_{2,42}$=41.16, p=0.00, two-way ANOVA with Bonferroni posttest). **e** Summary showing that density of long-thin spines was increased in cocaine-exposed rats, but decreased in morphine-exposed rats, and these effects were prevented by co-administration of GluA2$_{3Y}$ ($F_{2,42}$=32.56, p=0.00, two-way ANOVA with Bonferroni posttest). **f** Summary showing that density of stubby spines in cocaine- or morphine-exposed rats ($F_{2,42}$=6.94, p=0.00, two-way ANOVA). Error bar=s.e.m., *p<0.05, and **p<0.01.

Figure 5. Drug-induced alterations in spine morphology of mouse NAc MSNs

a–f: 1d withdrawal. **a** Example NAcSh dendrites from saline (n=16 mice)-, cocaine (n=21 mice)-, or morphine (n=25 mice)-exposed mice with or without co-administration of peptides. **b** Summary showing that density of total spines was increased in cocaine-exposed mice ($F_{2,53}$=62.09, p=0.00). **c** Summary showing that density of filopodia-like spines was increased in cocaine- and morphine-exposed mice, and morphine-induced increase was prevented by $GluA2_{3Y}$ co-administration ($F_{2,53}$=87.71, p=0.00). **d** Summary showing that density of mushroom-like spines was not affected in cocaine- or morphine-exposed mice ($F_{2,53}$=4.42, p=0.02). **e** Summary showing that density of long-thin spines was increased in cocaine-exposed mice ($F_{2,53}$=31.49, p=0.00). **f** Summary showing that the density of stubby spines was not altered in any experimental group ($F_{2,53}$=0.81, p=0.45). **g–l:** 21d withdrawal. **g** Example NAcSh dendrites from saline (n=13 mice)-, cocaine (n=15 mice)-, or morphine (n=17 mice)-exposed mice. **h** Summary showing that density of total spines was increased in cocaine-exposed mice, but decreased in morphine-exposed mice, and $GluA2_{3Y}$ co-administration prevented the morphine effects ($F_{2,36}$=60.97, p=0.00). **i** Summary showing that density of filopodia-like spines was not affected in cocaine- or morphine-exposed mice

($F_{2,36}$=0.33, p=0.72). **j** Summary showing that density of mushroom-like spines was increased in cocaine-exposed mice ($F_{2,36}$=20.65, p=0.00). **k** Summary showing that density of long-thin spines was increased in cocaine-exposed mice ($F_{2,36}$=37.17, p=0.00). **l** Summary showing that density of stubby spines was not altered in any experimental group ($F_{2,36}$=1.03, p=0.37). Two-way ANOVA with Bonferroni posttest was used in all above statistics. Error bar=s.e.m., *p<0.05, and **p<0.01.
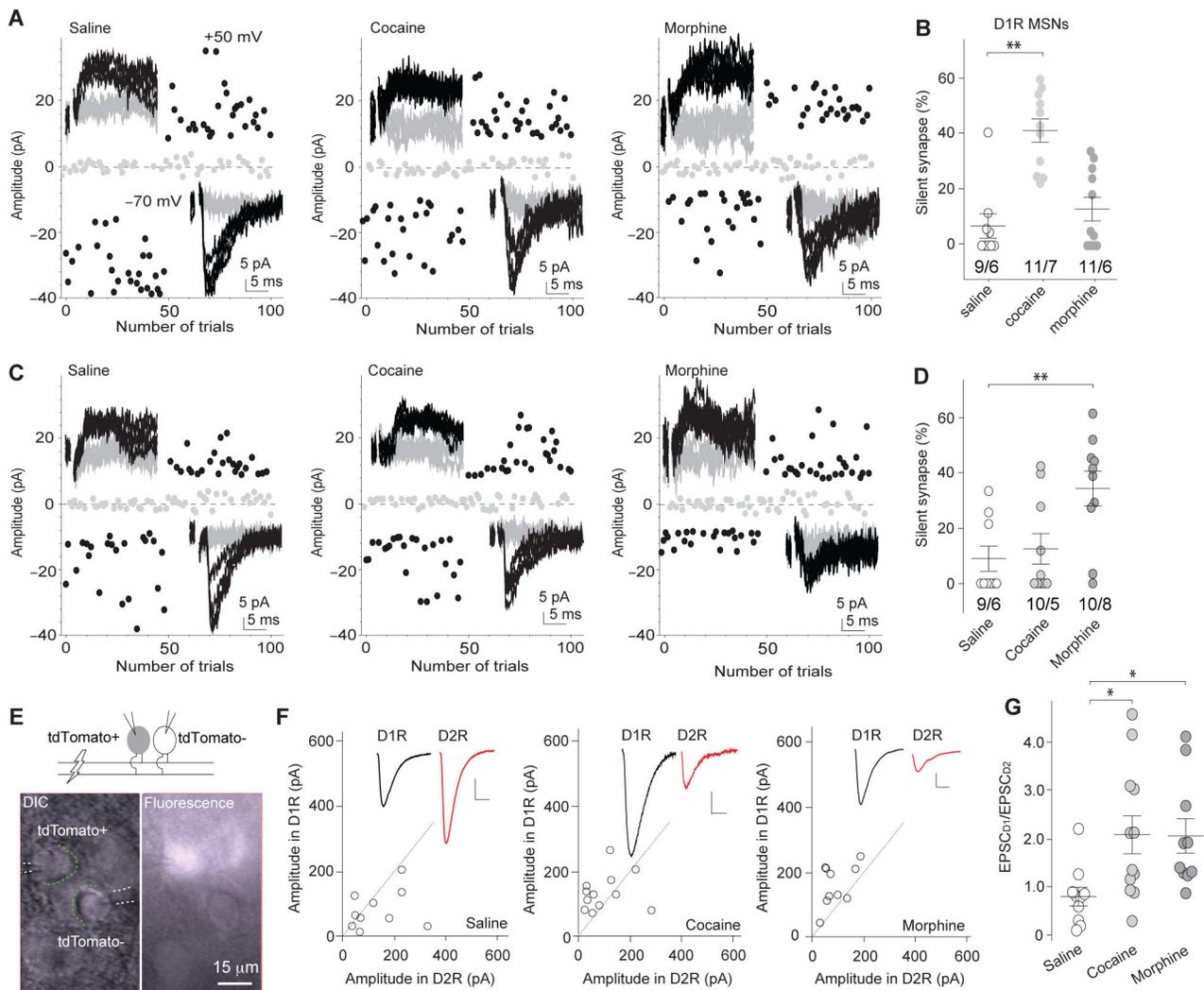
Figure 6. Cell type-specific generation of silent synapses after exposure to cocaine or morphine remodels excitatory circuits in the NAc

a Example EPSCs evoked by minimal stimulations and their trial plots in D1R NAcSh MSNs from mice 1d after saline (n=9/6 cells/mice), cocaine (n=11/7 cells/mice), or morphine (n=11/6 cells/mice) administration. **b** Summary showing that exposure to cocaine, but not morphine, generated silent synapses in D1R NAcSh MSNs ($F_{2,28}$=18.42, p=0.00, one-way ANOVA with Bonferroni posttest). **c** Example EPSCs evoked by minimal stimulations and their trial plots in D2R NAcSh MSNs from mice 1d after saline (n=9/6 cells/mice), cocaine (n=10/5 cells/mice), or morphine (n=10/8 cells/mice) administration. **d** Summary showing that exposure to morphine, but cocaine, generated silent synapses in D2R NAcSh MSNs ($F_{2,26}$=6.14, p=0.01, one-way ANOVA with Bonferroni posttest). **e** Illustration and images of dual recordings (n=32/9 slices/mice), in which the same stimulation-evoked EPSCs were simultaneously sampled from neighboring tdTomato+ and tdTomato- neurons. **f** Peak amplitudes of EPSCs in D1R MSNs plotted against those of simultaneously recorded in neighboring D2R MSNs in saline (n=10/3 slices/mice)-, cocaine (12/3 slices/mice)-, and morphine (10/3 slices/mice)-exposed mice 21–28d after saline/drug

administration. Insets, EPSCs in D1R (black) and D2R MSNs (red). Scale bars: 50pA, 5ms. **g** Summary showing the ratio of EPSC amplitudes in D1R MSNs over D2R MSNs ($EPSC_{D1}/EPSC_{D2}$) was similarly increased 21–28d after cocaine and morphine administration ($F_{2,29}=4.57$, $p=0.02$, one-way ANOVA with Bonferroni posttest). Error bar=s.e.m., *$p<0.05$, and **$p<0.01$.
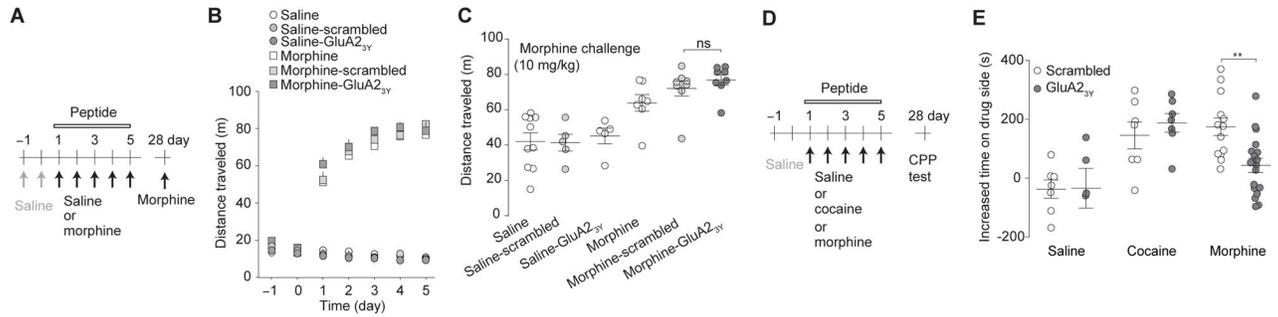
Figure 7. Intra-NAc infusion of GluA2$_{3Y}$ peptide selectively impairs the retention of morphine-induced CPP

a Time line and drug regimen of the locomotor procedure. On d-1 and d0, locomotor activity was measured in mice following saline injections. On d1–5, locomotor activity was measured following co-administration of GluA2$_{3Y}$ or scrambled peptide (1.5nm/g, iv) with saline or morphine (10mg/kg). Mice were kept in their homecages d6–27. On d28, saline- or cocaine-exposed mice received a challenge injection of morphine (10mg/kg) without co-administration of peptides. **b** Summary showing that co-administration of GluA2$_{3Y}$ did not affect morphine-induced locomotor responses over the 5d morphine procedure ($F_{12,120}$=0.89, p=0.56, two-way ANOVA). **c** Summary showing that GluA2$_{3Y}$ co-administration during the 5d morphine procedure did not affect morphine challenge-induced locomotor responses on d28 ($F_{5,37}$=12.87, p=0.00, one-way ANOVA with Bonferroni posttest). **d** Time line and drug regimen of the CPP procedure. **e** Summary showing that intra-NAcSh administration of GluA2$_{3Y}$ during the 5d drug procedure disrupted morphine-induced CPP without affecting cocaine-induced CPP tested 21d after conditioning ($F_{2,51}$=7.28, p=0.00, one-way ANOVA with Bonferroni posttest). Error bar=s.e.m., *p<0.05, and **p<0.01.